An extended hindered-rotor model with incorporation of Coriolis and vibrational-rotational coupling for calculating partition functions and derived quantities

P. Vansteenkiste,[a] D. Van Neck, V. Van Speybroeck, and M. Waroquier[b]
Laboratory of Theoretical Physics, Center for Molecular Modeling, Ghent University, Proeftuinstraat 86, B-9000 Gent, Belgium

(Received 20 May 2005; accepted 2 December 2005; published online 26 January 2006; publisher error corrected 28 April 2006)

Large-amplitude motions, particularly internal rotations, are known to affect substantially thermodynamic functions and rate constants of reactions in which flexible molecules are involved. Up to now all methods for computing the partition functions of these motions rely on the Pitzer approximation of more than 50 years ago, in which the large-amplitude motion is treated in complete independence of the other (vibrational) degrees of freedom. In this paper an extended hindered-rotor model (EHR) is developed in which the vibrational modes, treated harmonically, are correctly separated from the large-amplitude motion and in which relaxation effects (the changes in the kinetic-energy matrix and potential curvature) are taken into account as one moves along the large-amplitude path. The model also relies on a specific coordinate system in which the Coriolis terms vanish at all times in the Hamiltonian. In this way an increased level of consistency between the various internal modes is achieved, as compared with the more usual hindered-rotor (HR) description. The method is illustrated by calculating the entropies and heat capacities on 1,3-butadiene and 1-butene (with, respectively, one and two internal rotors) and the rate constant for the addition reaction of a vinyl radical to ethene. We also discuss various variants of the one-dimensional hindered-rotor scheme existing in the literature and its relation with the EHR model. It is argued why in most cases the HR approach is already quite successful. © *2006 American Institute of Physics*. [DOI: 10.1063/1.2161218]

I. INTRODUCTION

In standard *ab initio* calculations the molecular partition function, from which all thermodynamic molecular properties can be derived, is constructed using the independent harmonic-oscillator (HO) approximation. This description is adequate when only small deviations from the equilibrium geometry are relevant (i.e., low temperatures or steep potentials). Basically the HO model only needs information which can be derived from the equilibrium geometry. The low vibrational spectrum of most molecules is characterized by some large-amplitude vibrations that give rise to large deviations from the equilibrium configuration. Among them internal rotations (IR) about single bonds are certainly the most important. They have been the subject of extensive studies in the literature for decades. As the shape of the rotational potential gives rise to various stable conformers, the consideration of a quadratic form of the potential (as harmonic oscillator) is no longer meaningful and can lead to partition functions which largely deviate from the real ones. Instead of the HO approach one often applies a variant of the hindered-rotor (HR) model.

This HR model is usually implemented in one dimension (1D-HR). The potential energy becomes a function in the selected coordinate and may generate multiple local energy minima (conformers). Initially this potential energy was calculated as a rigid rotation, but nowadays it is obtained from a potential-energy scan in which the geometry is allowed to relax. The kinetic energy is completely determined by the moments of inertia, but the method of calculating the latter varies in different approximative schemes.

The simplest approximation was suggested by Pitzer[1–6] and has become a method of general use for one-dimensional treatment of internal rotors. Only the coupling with the overall rotation is taken into account, and neither relaxation effects nor coupling with other internal modes are involved. The calculation of the moments of inertia is based on the reference geometry, and it is further assumed that these moments remain fixed along the large-amplitude path. Despite the apparent inconsistency between the kinetic energy (with fixed moments of inertia) and the variable potential energy, this method led to good predictions for the entropy and heat capacity of *n*-alkanes.[7]

Pitzer also suggested a multidimensional treatment of the rotors. We applied this scheme (*n*D-HR) for pentane and hexane,[8,9] making use of the classical expression for the partition function as elaborated by Eidinoff and Aston.[10] At this stage the reduced moments of inertia are constructed from the full kinetic-energy matrix of the overall rotation and subsequent internal rotors, and represent functions of the rotational angles. This scheme represents a step forward in a more advanced and consistent description of IRs as the coupling between the overall rotation and internal rotors is taken

[a]Electronic mail: peter.vansteenkiste@ugent.be
[b]Author to whom correspondence should be addressed. Electronic mail: michel.waroquier@ugent.be

into account, but the coupling between internal rotations and other vibrations in the molecule is still ignored.

An overview of the several possibilities to construct (reduced) moments is given by East and Radom.[11]

Although the HR method can easily be implemented, this procedure still has some practical drawbacks.[12] For the calculation of molecular properties all vibrational modes are needed, whereas the HR method is applied only to some specific large-amplitude motions and thus does not provide a full description. The other vibrational modes are still treated with the HO method. Usually one replaces the harmonic modes corresponding to the internal rotation by its HR description, but the identification of these HO modes may be problematic for larger molecules since most of the low vibrational normal modes are mixtures of several internal rotations and other vibrations. A good illustration is the propagation kinetics of polyethylene in which large alkyl chains are involved (Scheme 1).

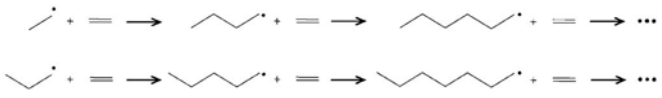

In these long-chain molecules no clear identification of separate internal rotations is possible due to a strong mixing among torsional modes and other skeletal vibrations.[13] It was shown that the 1D-HR model fails dramatically when used in conjunction with the HO frequencies obtained as output of a standard *ab initio* calculation. The propagation rate constant diverges for an increasing length of the alkyl chain, whereas all experiments point to a convergent behavior. The problem can be solved in a computationally attractive way by using one-dimensional HO predictions $q_{\mathrm{HO}}^{\mathrm{1D}}$ that are obtained using the second derivative of the rotational potential at the equilibrium position along the one-dimensional (1D) path of the torsional angle. However, the method is still not fully consistent, in the sense that the normal mode found by solving the complete multidimensional normal-mode problem differs from the one-dimensional solution.

In Ref. 12 of Ayala and Schlegel, a method is presented for the identification and treatment of internal rotations in a normal-mode vibrational analysis. A commonly committed error is that normal modes are inspected in terms of Cartesian coordinates instead of internal coordinates, frequently yielding wrong information. Ayala and Schlegel proposed a method for correcting these effects. They constructed a projector that removes all internal coordinates corresponding to bond stretches and bond angles, leaving only bond torsions (IRs). Then the normal-mode problem is solved yielding the projected vibrational frequencies and corresponding HO partition functions. Replacing these last values by those predicted by the IRs, an important correction is obtained for the partition function, and a valuable step is made in a consistent treatment of IRs and their impact on thermodynamic properties.

To some extent this model removes the inconsistency involved in the commonly used correction factor $q_{\mathrm{HR}}^{\mathrm{1D}}/q_{\mathrm{HO}}^{m\mathrm{D}}$ for the partition function, where $q_{\mathrm{HO}}^{m\mathrm{D}}$ corresponds to the normal mode found by solving the complete multidimensional normal-mode problem. This can give rise to large inaccuracies since the multidimensional solution differs from the one-dimensional mode: $q_{\mathrm{HO}}^{\mathrm{1D}} \neq q_{\mathrm{HO}}^{m\mathrm{D}}$. The determination of the one-dimensional HO prediction $q_{\mathrm{HO}}^{\mathrm{1D}}$ of the partition function of the vibrational mode which is replaced by an IR, also requires the calculation of the *effective* moment of inertia, more specifically the same moment as for the evaluation of $q_{\mathrm{HR}}^{\mathrm{1D}}$. Clearly, it should be useful to have a method that treats all low vibrational modes without inconsistencies or the need for *ad hoc* factors.

In addition to the problem of large-amplitude vibrations, much attention has been devoted to include rotational-vibrational coupling within the same framework. These approaches focus on the calculation of energy levels and are all based on the work of Watson.[14] In particular, we mention the work of Carter *et al.*[15] and Gerber and co-workers.[16] In these procedures, the Coriolis coupling terms add crucially to the complexity of the description and are usually ignored.

In 1989 Jellinek and Li emphasized the problem of separability of the global rotation and internal motion and proposed an exact description in which there exists a complete instantaneous separation of energies such that the Coriolis term in the Hamiltonian is zero at all times.[17] Our implementation as proposed in the current paper turns out to coincide with the principles of the Jellinek description. A general *Z*-matrix-like internal coordinate system ($3N-6$ variables) is introduced and connected with the global variables (translation, global rotation) by imposing appropriate conditions. These are conservation of momentum and angular momentum under internal reorganization.

In practice, one needs to introduce two body-fixed frames: (i) frame (1) coinciding with the center of mass (at all times) and representing the global motion and (ii) frame (2) attached to the reference atoms chosen for determining the internal coordinates. Frame (1) is defined in such a way that the atomic velocities in this frame do not contribute to the total linear and angular momenta of the system. The resulting classical description of the kinetic energy will be derived in the next section.

In the second part of the theory, an extended HR (EHR) description is introduced which is based on the exact (classical) kinetic-energy description in combination with an appropriate approximation of the potential energy for one internal rotor. The rotational potential is written as a one-dimensional function $V^{\mathrm{HR}}(\varphi)$, as usually done in the standard HR model, but in the other $3N-7$ coordinates (orthogonal to the large-amplitude path) a quadratic approximation is used resulting in a φ-dependent Hessian for the vibrational degrees of freedom. Since our main interest goes to the accurate determination of thermodynamic and kinetic quantities derived from the partition function, the whole scheme is solved classically except for the small-amplitude vibrations that are treated quantum mechanically. The classical solution implies that the traditional interpretation of the energy levels is given up.

The proposed EHR model has the merit of a consistent

treatment of the harmonic-oscillator and hindered-rotor descriptions, integrated in one unified model, and also fully incorporates the variation of the geometry by means of variable (internal and principal) moments of inertia for all modes.

In this paper we also examine how the global partition function in the 1D-HR scheme is related to its EHR counterpart, and why the former yields good results in most of the cases.

The EHR model will be validated on its capability of reproducing thermodynamic quantities such as entropy and heat capacity in 1,3-butadiene, in which only one rotor is present and for which experimental data are available. The EHR model is easily extended to multiple internal rotors. This is demonstrated on 1-butene, in which two internal rotors are present.

Another quantity of interest is the frequency factor of the reaction rate. The reaction rate is directly proportional to the partition function of the transition state. In the case of addition reactions, for example, the rate is sensitive to the details of the description of the additional internal rotation about the forming bond. The importance of internal rotations in the transition state is well documented in the literature for addition reactions of radicals to olefins.[18,19] In this paper we demonstrate the impact of coupling with the other vibrational modes on the addition of a vinyl radical to ethene.

II. THEORY

A. Classical kinetic energy

In order to derive the classical kinetic energy for a molecule with N atoms, one needs to introduce appropriate variables of motion. In a Z-matrix-like formulation, it is possible to define $n=3N-6$ internal coordinates θ_i, describing the internal structure of the molecule related to a frame B' that is determined by the first three atoms. The absolute position of atom 1 is taken as the origin $O_{B'}$, while the vector $\boldsymbol{r}_{12}$ between atoms 1 and 2 determines the $X_{B'}$ axis and the component of $\boldsymbol{r}_{23}$ perpendicular to this axis determines the $Y_{B'}$ axis.

In this way, the coordinates of atom A in the space-fixed frame S are described by the vector:

$$\boldsymbol{r}_A^{(S)} = \boldsymbol{r}_{O_{B'}}^{(S)} + \bar{R}_{B'S} \cdot \boldsymbol{r}_A^{(B')}(\theta_i), \tag{1}$$

where $\bar{R}_{B'S}$ is the rotational tensor between the orientation of the axes in frames B' and S. It is convenient to introduce an additional frame B that at a given time ($t=0$) coincides with the center of mass (c.m.) and is oriented along the principal axes of the molecule, but with as yet unspecified dynamics. The coordinates in frame S can be expressed as

$$\boldsymbol{r}_A^{(S)} = \boldsymbol{r}_{O_B}^{(S)} + \bar{R}_{BS} \cdot \boldsymbol{r}_A^{(B)} = \boldsymbol{r}_{O_B}^{(S)} + \bar{R}_{BS} \cdot (\boldsymbol{r}_{O_{B'}}^{(B)} + \bar{R}_{B'B} \cdot \boldsymbol{r}_A^{(B')}(\theta_i)), \tag{2}$$

and the velocity of atom A in the S frame becomes

$$\dot{\boldsymbol{r}}_A^{(S)} = \dot{\boldsymbol{r}}_{O_B}^{(S)} + \dot{\bar{R}}_{BS} \cdot \boldsymbol{r}_A^{(B)} + \bar{R}_{BS} \cdot (\dot{\boldsymbol{r}}_{O_{B'}}^{(B)} + \dot{\bar{R}}_{B'B} \cdot \boldsymbol{r}_A^{(B')} + \bar{R}_{B'B} \cdot \dot{\boldsymbol{r}}_A^{(B')}). \tag{3}$$

The velocity of atom A in the B' frame has the generic form

$$\dot{\boldsymbol{r}}_A^{(B')} = \sum_i \frac{\partial \boldsymbol{r}_A^{(B')}}{\partial \theta_i} \dot{\theta}_i = \sum_i \boldsymbol{U}_i^{(B')}(A)\,\dot{\theta}_i. \tag{4}$$

For practical calculations, the n internal coordinates in the Z-matrix formalism can be divided into three classes: dihedral angle, bond angle, or bond length.

(i) The first two classes correspond with rotations about an axis lying along a bond (changes in dihedral) or about an axis perpendicular to the plane formed by two bonds (changes in bond angle). The velocity (in frame B') of atom A subject to these two rotations can be expressed in terms of an angular velocity $\boldsymbol{\omega}_i$ as follows:

$$\boldsymbol{U}_i^{(B')}(A)\,\dot{\theta}_i = \boldsymbol{\omega}_i^{(B')} \times (\boldsymbol{r}_A^{(B')} - \boldsymbol{r}_{O_i}^{(B')}) = \bar{\chi}^{(B')}(A - O_i) \cdot \boldsymbol{\omega}_i^{(B')}, \tag{5}$$

where O_i is the origin of the rotation (lies on the $\boldsymbol{\omega}_i$ axis), and $\bar{\chi}^{(B')}$ represents a tensor with matrix representation

$$\bar{\chi}^{(B')}(A - O_i) = \begin{bmatrix} 0 & +(z_A^{(B')} - z_{O_i}^{(B')}) & -(y_A^{(B')} - y_{O_i}^{(B')}) \\ -(z_A^{(B')} - z_{O_i}^{(B')}) & 0 & +(x_A^{(B')} - x_{O_i}^{(B')}) \\ +(y_A^{(B')} - y_{O_i}^{(B')}) & -(x_A^{(B')} - x_{O_i}^{(B')}) & 0 \end{bmatrix} \tag{6}$$

for any atom A submitted to this rotation. It is equal to zero for any other atom A. The unit vector of the angular velocity $\boldsymbol{\omega}_i^{(B')} = \boldsymbol{e}_{\omega_i}^{(B')}(\theta_1, \ldots, \theta_n)\,\dot{\theta}_i$ depends on the internal geometry.

(ii) The third class of internal coordinates corresponds to a bond stretch and results in a constant contribution to the velocity

$$\boldsymbol{U}_i^{(B')}(A)\,\dot{\theta}_i = \boldsymbol{v}_i^{(B')} = \boldsymbol{e}_{v_i}^{(B')}(\theta_1, \ldots, \theta_n)\,\dot{\theta}_i. \tag{7}$$

Note that $\boldsymbol{U}_i^{(B')}(A)$ represents a vector and that a transformation to any other frame is accordingly given by $\boldsymbol{U}_i^{(S)}(A) = \bar{R}_{B'S} \cdot \boldsymbol{U}_i^{(B')}(A)$.

The time derivatives of the rotation tensors appearing in Eq. (3) can be reformulated, using $\bar{\chi}$ tensors, as

$$\dot{\bar{R}}_{BS} \cdot \boldsymbol{r}_A^{(B)} = \bar{\chi}^{(S)}(A - O_B) \cdot \boldsymbol{\omega}^{(S)}, \tag{8}$$

$$\dot{\bar{R}}_{B'B} \cdot \boldsymbol{r}_A^{(B')} = \bar{\chi}^{(B)}(A - O_{B'}) \cdot \boldsymbol{\nu}^{(B)}, \tag{9}$$

where we introduced two rotation vectors $\boldsymbol{\omega}^{(S)}$ and $\boldsymbol{\nu}^{(B)}$ controlling the rotation of frame B relative to S and of frame B' relative to B.

The velocity of atom A can now be written as

$$\dot{\boldsymbol{r}}_A^{(S)} = \dot{\boldsymbol{r}}_{O_B}^{(S)} + \bar{\chi}^{(S)}(A - O_B) \cdot \boldsymbol{\omega}^{(S)} + \bar{R}_{BS} \cdot \dot{\boldsymbol{r}}_A^{(B)}, \tag{10}$$

$$\dot{\boldsymbol{r}}_A^{(B)} = \dot{\boldsymbol{r}}_{O_{B'}}^{(B)} + \bar{\chi}^{(B)}(A - O_{B'}) \cdot \boldsymbol{\nu}^{(B)} + \sum_i \boldsymbol{U}_i^{(B)}(A)\dot{\theta}_i. \tag{11}$$

In this expression the relative motion of B and B' is described by the vectors $\dot{\boldsymbol{r}}_{O_{B'}}^{(B)}$ and $\boldsymbol{\nu}^{(B)}$ and can be eliminated by imposing suitable conditions on the B frame. Apart from the initial conditions at $t=0$, the dynamics of the B frame is at this point still unspecified. In the simple case of a rigid body, frame B' is fixed to B and the angular velocity $\boldsymbol{\nu}^{(B)}$ disappears. Only one contribution remains [terms with $\boldsymbol{\omega}^{(S)}$] describing the overall rotation of the molecule. In the present case of a nonrigid molecule, we still would like frame B to refer exclusively to the overall rotation (and translation), by imposing certain conditions on its dynamics. In particular, we impose that the total momentum and angular momentum of the molecule are vanishing in frame B:

$$\sum_A m_A \dot{\boldsymbol{r}}_A^{(B)} = 0, \tag{12}$$

$$\sum_A m_A \boldsymbol{r}_A^{(B)} \times \dot{\boldsymbol{r}}_A^{(B)} = 0. \tag{13}$$

In addition to these constraints we assume that the origin of frame B coincides at $t=0$ with the c.m. The first condition (12) leads to $\boldsymbol{r}_{\text{c.m.}}^{(B)} = \Sigma_A m_A \boldsymbol{r}_A^{(B)}/M = 0$ for all times t and ensures that the origin of frame B remains in the c.m. From Eq. (2) it then follows that $\boldsymbol{r}_{O_B}^{(S)} = \boldsymbol{r}_{\text{c.m.}}^{(S)}$. Deriving the c.m. velocity from Eq. (11),

$$\begin{aligned} M\dot{\boldsymbol{r}}_{\text{c.m.}}^{(S)} &= \sum_A m_A \dot{\boldsymbol{r}}_A^{(S)} \\ &= M\dot{\boldsymbol{r}}_{O_B}^{(S)} + \bar{\chi}^{(S)}\left(\sum_A m_A \boldsymbol{r}_A^{(S)} - M\boldsymbol{r}_{O_B}^{(S)}\right) \cdot \boldsymbol{\omega}^{(S)} \\ &\quad + \bar{R}_{BS} \cdot \left[M\dot{\boldsymbol{r}}_{O_{B'}}^{(B)} + \bar{\chi}^{(B)}\left(\sum_A m_A \boldsymbol{r}_A^{(B)} - M\boldsymbol{r}_{O_{B'}}^{(B)}\right) \cdot \boldsymbol{\nu}^{(B)} \right. \\ &\quad \left. + \sum_i \sum_A m_A \boldsymbol{U}_i^{(B)}(A)\dot{\theta}_i \right] \end{aligned} \tag{14}$$

It is clear that condition (12) is equivalent to

$$\dot{\boldsymbol{r}}_{O_{B'}}^{(B)} = -\bar{\chi}^{(B)}(-O_{B'}) \cdot \boldsymbol{\nu}^{(B)} - \frac{1}{M}\sum_i \left(\sum_A m_A \boldsymbol{U}_i^{(B)}(A)\right)\dot{\theta}_i. \tag{15}$$

Defining, for each internal coordinate, $\boldsymbol{W}_i^{(B)} = \Sigma_A m_A \boldsymbol{U}_i^{(B)}(A)$, one may rewrite the velocity of atom A as

$$\dot{\boldsymbol{r}}_A^{(S)} = \dot{\boldsymbol{r}}_{\text{c.m.}}^{(S)} + \bar{\chi}^{(S)}(A - \text{c.m.}) \cdot \boldsymbol{\omega}^{(S)} + \bar{R}_{BS} \cdot \dot{\boldsymbol{r}}_A^{(B)},$$

$$\dot{\boldsymbol{r}}_A^{(B)} = \bar{\chi}^{(B)}(A) \cdot \boldsymbol{\nu}^{(B)} + \sum_i \left(\boldsymbol{U}_i^{(B)}(A) - \frac{1}{M}\boldsymbol{W}_i^{(B)}\right)\dot{\theta}_i. \tag{16}$$

This means that the "freedom" of rotation of frame B' relative to B is restricted to rotation axes through the origin of B or, equivalently, the center of mass. Also, there is a correction to $\boldsymbol{U}_i$ in order to keep the center of mass at O_B.

The remaining unknown quantity $\boldsymbol{\nu}^{(B)}$ is determined by the angular momentum condition (13). Using the $\bar{\chi}$ tensor formulation, this constraint is rewritten as

$$\sum_A m_A \boldsymbol{r}_A^{(B)} \times \dot{\boldsymbol{r}}_A^{(B)} = -\sum_A m_A \bar{\chi}^{(B)}(A) \cdot \dot{\boldsymbol{r}}_A^{(B)} = 0. \tag{17}$$

Replacing $\dot{\boldsymbol{r}}_A^{(B)}$ with Eq. (16), we get

$$\begin{aligned} &\sum_A m_A \bar{\chi}^{(B)}(A) \cdot \left(\bar{\chi}^{(B)}(A) \cdot \boldsymbol{\nu}^{(B)}\right) \\ &\quad = -\sum_i \sum_A m_A \bar{\chi}^{(B)}(A) \cdot \left(\boldsymbol{U}_i^{(B)}(A) - \frac{1}{M}\boldsymbol{W}_i^{(B)}\right)\dot{\theta}_i. \end{aligned} \tag{18}$$

This leads to the determination of the angular velocity $\boldsymbol{\nu}^{(B)}$ in terms of the inertial tensor $\bar{I}$,

$$\boldsymbol{\nu}^{(B)} = -\sum_i \left(\bar{I}^{(B)}\right)^{-1} \cdot \boldsymbol{X}_{0i}^{(B)}\dot{\theta}_i, \tag{19}$$

with

$$\bar{X}_{00}^{(B)} = \sum_A m_A \bar{\chi}^{(B)}(A) \cdot \bar{\chi}^{(B)}(A) = \bar{I}^{(B)},$$

$$\boldsymbol{X}_{0i}^{(B)} = \sum_A m_A \bar{\chi}^{(B)}(A) \cdot \boldsymbol{U}_i^{(B)}(A).$$

The final expression for the velocity of atom A reads

$$\begin{aligned} \dot{\boldsymbol{r}}_A^{(S)} &= \dot{\boldsymbol{r}}_{\text{c.m.}}^{(S)} + \bar{\chi}^{(S)}(A - \text{c.m.}) \cdot \boldsymbol{\omega}^{(S)} + \sum_i \left(\boldsymbol{U}_i^{(S)}(A) - \frac{1}{M}\boldsymbol{W}_i^{(S)}\right. \\ &\quad \left. - \bar{\chi}^{(S)}(A - \text{c.m.}) \cdot (\bar{I}^{(S)})^{-1} \cdot \boldsymbol{X}_{0i}^{(S)}\right)\dot{\theta}_i. \end{aligned} \tag{20}$$

An interesting feature to note is that the B frame turns out to coincide exactly with the frame introduced by Jellinek and Li,[17] but based upon different grounds. It is easy to show, for example, that by virtue of Eqs. (13) and (16), the total angular momentum with respect to the c.m.,

$$\begin{aligned} \boldsymbol{L}^{(S)} &= \sum_A m_A (\boldsymbol{r}_A^{(S)} - \boldsymbol{r}_{\text{c.m.}}^{(S)}) \times (\dot{\boldsymbol{r}}_A^{(S)} - \dot{\boldsymbol{r}}_{\text{c.m.}}^{(S)}) \\ &= \sum_A m_A (\boldsymbol{r}_A^{(S)} - \boldsymbol{r}_{\text{c.m.}}^{(S)}) \times [\boldsymbol{\omega}^{(S)} \times (\boldsymbol{r}_A^{(S)} - \boldsymbol{r}_{\text{c.m.}}^{(S)})] \\ &= \bar{I}^{(S)} \cdot \boldsymbol{\omega}^{(S)}, \end{aligned} \tag{21}$$

is at each instant the same as that of a rigid body with inertial tensor $\bar{I}$ and angular velocity $\boldsymbol{\omega}^{(S)}$.

The kinetic energy $T = 1/2 \Sigma_A m_A \dot{\boldsymbol{r}}_A^{(S)} \cdot \dot{\boldsymbol{r}}_A^{(S)}$ can now be worked out as

$$T=\frac{1}{2}\boldsymbol{\omega}\cdot\bar{I}\cdot\boldsymbol{\omega}+\frac{M}{2}(\dot{\boldsymbol{r}}_{\mathrm{c.m.}})^2+\frac{1}{2}\sum_i\sum_j\dot{\theta}_i\dot{\theta}_j\Big(X_{ij}-\boldsymbol{W}_i\cdot\frac{1}{M}\boldsymbol{W}_j-\boldsymbol{X}_{0i}\cdot\bar{I}^{-1}\cdot\boldsymbol{X}_{0j}-\frac{1}{M}\boldsymbol{W}_i\cdot\boldsymbol{W}_j+\frac{M}{M^2}\boldsymbol{W}_i\cdot\boldsymbol{W}_j$$
$$+\frac{1}{M}\boldsymbol{W}_i\cdot M\bar{\chi}(\mathrm{c.m.}-\mathrm{c.m.})\cdot\bar{I}^{-1}\cdot\boldsymbol{X}_{0j}-\boldsymbol{X}_{0i}\cdot\bar{I}^{-1}\cdot\boldsymbol{X}_{0j}+\boldsymbol{X}_{0i}\cdot\bar{I}^{-1}\cdot M\bar{\chi}(\mathrm{c.m.}-\mathrm{c.m.})\cdot\frac{1}{M}\boldsymbol{W}_j+\boldsymbol{X}_{0i}\cdot\bar{I}^{-1}\cdot\bar{I}\cdot\bar{I}^{-1}\cdot\boldsymbol{X}_{0j}\Big)$$
$$+M\dot{\boldsymbol{r}}_{\mathrm{c.m.}}\cdot\bar{\chi}(\mathrm{c.m.}-\mathrm{c.m.})\cdot\boldsymbol{\omega}+M\dot{\boldsymbol{r}}_{\mathrm{c.m.}}\cdot\sum_i\left(\frac{1}{M}\boldsymbol{W}_i-\frac{1}{M}\boldsymbol{W}_i-\bar{\chi}(\mathrm{c.m.}-\mathrm{c.m.})\cdot\bar{I}^{-1}\cdot\boldsymbol{X}_{0i}\right)\dot{\theta}_i$$
$$+\boldsymbol{\omega}\cdot\sum_i\left(\boldsymbol{X}_{0i}-\bar{\chi}(\mathrm{c.m.}-\mathrm{c.m.})\cdot\boldsymbol{W}_i-\bar{I}\cdot\bar{I}^{-1}\cdot\boldsymbol{X}_{0i}\right)\dot{\theta}_i, \tag{22}$$

with the additional definition

$$X_{ij}=\sum_A m_A\boldsymbol{U}_i(A)\cdot\boldsymbol{U}_j(A). \tag{23}$$

In the above expression many contributions cancel each other, and the final result is simply

$$T=\frac{1}{2}\boldsymbol{\omega}\cdot\bar{I}\cdot\boldsymbol{\omega}+\frac{M}{2}(\dot{\boldsymbol{r}}_{\mathrm{c.m.}})^2+\frac{1}{2}\sum_i\sum_j(X_{ij}-\boldsymbol{W}_i\cdot M^{-1}\boldsymbol{W}_j$$
$$-\boldsymbol{X}_{0i}\cdot\bar{I}^{-1}\cdot\boldsymbol{X}_{0j})\dot{\theta}_i\dot{\theta}_j. \tag{24}$$

Note that no Coriolis contributions (terms of the form $\boldsymbol{\omega}\dot{\theta}_i$) are present in Eq. (24) and that all quantities involved are rotational scalars. In particular, the coefficients of the $\dot{\theta}_i\dot{\theta}_j$ terms only depend on the geometry, i.e., on the internal coordinate vector $\Theta=(\theta_1,\ldots,\theta_n)^T$. In matrix form, the internal part of the kinetic energy can therefore be written as

$$T_{\mathrm{int}}=\frac{1}{2}\dot{\Theta}^T A_\Theta(\theta_1,\ldots,\theta_n)\dot{\Theta}. \tag{25}$$

The expression of the kinetic energy [Eq. (24)] shows a separation between the internal motions and the overall rotation and translation. It can be argued that this is the only meaningful definition of internal motion when large-amplitude deviations from the equilibrium geometry are present. The drawback, of course, lies in the fact that $\boldsymbol{\omega}$ is a function of both the positions and velocities of the atoms, and cannot be defined as the time derivative of some generalized coordinate.

If one considers systems at definite angular momentum, the centrifugal term $\boldsymbol{\omega}\cdot\bar{I}\cdot\boldsymbol{\omega}/2=\boldsymbol{L}\cdot(\bar{I})^{-1}\cdot\boldsymbol{\omega}/2$ can be taken as an additional potential influencing the internal motion. For the present applications to partition functions and thermodynamic properties, we will only take the average effect of the centrifugal term into account in the total partition function. For the contribution of the internal modes we further concentrate on the system with $\boldsymbol{L}=0$.

B. Extended hindered-rotor (EHR) model

To illustrate the utility and efficiency of the extended hindered-rotor model we further elaborate on the case of one internal rotation. The presented theory can easily be extended to multiple large-amplitude motions.

If we define $\varphi=\theta_1$ to be the dihedral angle associated with the internal rotation, the potential-energy profile $V^{\mathrm{HR}}(\varphi)$ is a function of this coordinate only. The standard procedure to obtain $V^{\mathrm{HR}}(\varphi)$ is to perform a constrained optimization with the angle φ fixed at various values. This approach, in which all variables except φ are allowed to relax, yields the equilibrium values $\theta_i^{\mathrm{eq}}(\varphi)$ of the other variables as a function of φ. They may differ from the values of the internal coordinates θ_i corresponding to the most stable conformation $(\varphi=0)$ and the deviations

$$\tau_i=\theta_i-\theta_i^{\mathrm{eq}}(\varphi) \tag{26}$$

may be regarded as new coordinates. It is now a reasonable approximation to expand, for each value of φ, the potential-energy variation in the vibrational coordinates τ_i up to second order,

$$V^{\mathrm{tot}}(\varphi,\tau)=V^{\mathrm{HR}}(\varphi)+\frac{1}{2}\tau^T H^{\mathrm{vib}}(\varphi)\tau. \tag{27}$$

The matrix $H^{\mathrm{vib}}(\varphi)$ is the Hessian of the remaining vibrations as a function of φ. To the same level of approximation the kinetic matrix A_Θ in Eq. (25) should be evaluated along the large-amplitude path with $\theta_i=\theta_i^{\mathrm{eq}}(\varphi)$, and depends only on φ. Using the fact that

$$\dot{\tau}_i=\dot{\theta}_i-\frac{\partial\theta_i^{\mathrm{eq}}}{\partial\varphi}\dot{\varphi}, \tag{28}$$

the internal kinetic energy in the new variables becomes

$$T_{\mathrm{int}}=\frac{1}{2}\begin{bmatrix}\dot{\varphi} & \dot{\tau}^T\end{bmatrix}A(\varphi)\begin{bmatrix}\dot{\varphi}\\ \dot{\tau}\end{bmatrix}, \tag{29}$$

with the transformed kinetic-energy matrix given by

$$A(\varphi)=\begin{pmatrix}1 & \partial\theta_2^{\mathrm{eq}}/\partial\varphi & \cdots & \partial\theta_n^{\mathrm{eq}}/\partial\varphi\\ 0 & 1 & 0 & 0\\ \vdots & 0 & \ddots & \vdots\\ 0 & 0 & \cdots & 1\end{pmatrix}A_\Theta\begin{pmatrix}1 & 0 & \cdots & 0\\ \partial\theta_2^{\mathrm{eq}}/\partial\varphi & 1 & 0 & 0\\ \vdots & 0 & \ddots & \vdots\\ \partial\theta_n^{\mathrm{eq}}/\partial\varphi & 0 & \cdots & 1\end{pmatrix}=\begin{pmatrix}A_{\varphi\varphi} & A_{\varphi\tau}\\ A_{\tau\varphi} & A_{\tau\tau}\end{pmatrix}. \tag{30}$$

The total energy $E_{\mathrm{tot}}=E_{\mathrm{tr}}+E_{\mathrm{rot}}+E_{\mathrm{int}}$ can now be written as

$$E_{\mathrm{tr}}=\frac{1}{2}M(\dot{x}_{\mathrm{c.m.}}^2+\dot{y}_{\mathrm{c.m.}}^2+\dot{z}_{\mathrm{c.m.}}^2), \tag{31}$$

$$E_{\mathrm{rot}}=\frac{1}{2}\omega^T I(\varphi)\omega, \tag{32}$$

$$\begin{aligned}E_{\mathrm{int}}&=\frac{1}{2}\begin{bmatrix}\dot{\varphi} & \dot{\tau}^T\end{bmatrix}A(\varphi)\begin{bmatrix}\dot{\varphi}\\ \dot{\tau}\end{bmatrix}+V^{\mathrm{HR}}(\varphi)+\frac{1}{2}\tau^T H^{\mathrm{vib}}(\varphi)\tau\\ &=\frac{1}{2}\begin{bmatrix}p_\varphi & P_\tau^T\end{bmatrix}A^{-1}(\varphi)\begin{bmatrix}p_\varphi\\ P_\tau\end{bmatrix}+V^{\mathrm{HR}}(\varphi)+\frac{1}{2}\tau^T H^{\mathrm{vib}}(\varphi)\tau.\end{aligned} \tag{33}$$

The energy contribution E_{int} arising from the internal motions has been transformed into its canonical form with generalized coordinates (φ,τ) and moments (p_φ,P_τ).

At this point we distinguish between the "slow" internal rotation and the "fast" vibrations (having higher frequencies) by assuming that the latter follow adiabatically the geometrical changes due to the rotational motion. The rotational variables φ,p_φ are treated classically, whereas the τ,P_τ are considered as canonically conjugate quantum-mechanical operators (i.e., $P_{\tau_i}=-i\hbar\,\partial/\partial\tau_i$). In other words, E_{int} can be viewed as a quantum-mechanical Hamiltonian for the vibrations, with parametric dependence on φ,p_φ.

As indicated, we will only consider the averaged effect of the centrifugal term in Eq. (32) on the molecular partition function. It seems physically reasonable that this can be done (at the classical level) by integrating over all possible values of the angular momentum. The resulting contribution Q_{rot} to the partition function is that of a rigid body with inertial tensor $\bar{I}$, and as it is proportional to the determinant $\mathrm{Det}[I]$ it only depends on the internal geometry, $Q_{\mathrm{rot}}\equiv Q_{\mathrm{rot}}(\varphi,T)$, where T stands for the temperature.

Based on Eqs. (31)–(33) one can then propose the following expression for the molecular partition function (omitting the trivial translational part):

$$Q_{\text{rot-int}}(T)=\frac{1}{h}\int d\varphi Q_{\mathrm{rot}}(\varphi,T)dp_\varphi\,\mathrm{Tr}[\mathrm{e}^{-\beta E_{\mathrm{int}}}], \tag{34}$$

with $\beta=1/RT$, where the integration is over the phase space of the classical variables, and the trace is taken with respect to the Hilbert space of the τ,P_{τ_i} operators.

The trace can be evaluated exactly, since the eigenvalues of E_{int} are known. To see this, one notes that the vibrational Hamiltonian is of the generic form

$$\mathcal{H}=P_\tau^T BP_\tau+b^T P_\tau+P_\tau^T b+\tau^T C\tau, \tag{35}$$

where the positive-definite matrices B and C, as well as the column matrix b, are constant. To find the eigenvalue spectrum we may as well work in momentum space, treating the P_i as real numbers and the $\tau_i=+i\hbar\,\partial/\partial P_{\tau_i}$ as operators. The terms in Eq. (35) which are linear in P_τ can then be absorbed by a shift $P'_\tau=P_\tau+B^{-1}b$ in the P_{τ_i} variables, yielding

$$\mathcal{H}=P'^T_\tau BP'_\tau+\tau^T C\tau-b^T B^{-1}b. \tag{36}$$

The last term merely produces a constant shift in the eigenvalues, and since we still have that $\tau_i=+i\hbar\,\partial/\partial P'_{\tau_i}$, the Hamiltonian in Eq. (36) is now the standard representation of a system of HO which can be decoupled in the usual way. Application to Eq. (34) yields

$$\begin{aligned}Q_{\text{rot-int}}(T)=\int d\varphi e^{-\beta V^{\mathrm{HR}}(\varphi)}Q_{\mathrm{rot}}(\varphi,T)\prod_{i=2}^{n}Q_i^{\mathrm{HO}}(\varphi,T)\frac{1}{h}\int dp_\varphi\\ \times\exp\Bigg(-\frac{\beta p_\varphi^2}{2}[(A^{-1})_{\varphi\varphi}\\ -(A^{-1})_{\varphi\tau}[(A^{-1})_{\tau\tau}]^{-1}(A^{-1})_{\tau\varphi}]\Bigg),\end{aligned} \tag{37}$$

where the φ-dependent HO frequencies follow from $\mathrm{Det}[H^{\mathrm{vib}}-\omega_i A_{\tau\tau}]=0$. Also note that the subsequent p_φ integration does not need an explicit calculation of A^{-1}, since

$$(A^{-1})_{\varphi\varphi}-(A^{-1})_{\varphi\tau}[(A^{-1})_{\tau\tau}]^{-1}(A^{-1})_{\tau\varphi}=(A_{\varphi\varphi})^{-1}. \tag{38}$$

The same statement holds also for the case of more than one internal rotor.

The focus of this work is to compute the total partition function of a molecule. Contrary to the well-known HR model, the global rotational and vibrational parts are solved for each value of φ. All vibrational degrees of freedom, except for the "isolated" internal rotation, are treated quantum mechanically, whereas the hindered-rotor part and global rotation are solved classically by integration,

$$\begin{aligned}Q_{\mathrm{rot,int}}^{\mathrm{EHR}}=K(T)\int_0^{2\pi}d\varphi\sqrt{A_\varphi(\varphi)}e^{-\beta V^{\mathrm{HR}}(\varphi)}\\ \times\prod_{i=2}^{n}Q_i^{\mathrm{HO}}(\varphi,T)Q_{\mathrm{rot}}(\varphi,T),\end{aligned} \tag{39}$$

with $K(T)=\sqrt{2\pi k_B T/h^2}$. This classical solution is valid for high T, and the extension to lower temperatures is made by applying the Pitzer-Gwin correction $Q_\varphi^{\text{HO-QM}}/Q_\varphi^{\text{HO-Cl}}$.[2]

This leads to the final expression of the global partition function of the molecule within the scope of a consistent

scheme (EHR) in which both large- and small-amplitude vibrations are treated on the same footing. It is instructive to introduce a scaling factor $\kappa_{\mathrm{EHR}}(T)$ defined as the ratio between the true EHR partition function [Eq. (39)] and the HO prediction resulting from the standard *ab initio* programs, e.g., GAUSSIAN (Ref. 20) and others:

$$Q_{\mathrm{rot,int}}^{\mathrm{EHR}}(T) = \kappa_{\mathrm{EHR}}(T) Q_{\mathrm{rot,int}}^{\mathrm{HO}}(T). \tag{40}$$

The HO expression for the total partition function consists of the product of the global rotation partition function $Q_{\mathrm{rot}}(\varphi=0,T)$ and the total partition function of the internal modes in the HO approach, but determined at the global energy minimum (i.e., $\varphi=0$):

$$Q_{\mathrm{int}}^{\mathrm{HO}}(T) = \prod_{i=1}^{n} Q_i^{\mathrm{HO}}(\varphi=0,T). \tag{41}$$

This enables us to extract a closed expression for the scaling factor $\kappa_{\mathrm{EHR}}(T)$:

$$\kappa_{\mathrm{EHR}}(T) = c_\varphi \int_0^{2\pi} f_A(\varphi) f_{\mathrm{vib}}(\varphi,T) e^{-\beta V^{\mathrm{HR}}(\varphi)} d\varphi, \tag{42}$$

with the geometry correction factor:

$$f_A(\varphi) = \sqrt{\frac{A_\varphi(\varphi)}{A_\varphi(0)} \frac{I_x(\varphi) I_y(\varphi) I_z(\varphi)}{I_x(0) I_y(0) I_z(0)}}, \tag{43}$$

as originally introduced in Refs. 8 and 9, and the vibrational correction factor:

$$f_{\mathrm{vib}}(\varphi,T) = \frac{\prod_{i=2}^{n} Q_i^{\mathrm{HO}}(\varphi,T)}{\prod_{i=2}^{n} Q_i^{\mathrm{HO}}(0,T)}. \tag{44}$$

The coefficient

$$c_\varphi = \frac{1}{Q_{\varphi,\mathrm{Cl}}^{\mathrm{HO}}} K(T) \sqrt{A_\varphi(0)} \tag{45}$$

can further be elaborated yielding

$$c_\varphi = \sqrt{\frac{\beta}{2\pi}} \sqrt{\left.\frac{\partial^2 V}{\partial \varphi^2}\right|_0}, \tag{46}$$

and following closed expression for the correct EHR partition function is found:

$$\begin{aligned} Q_{\mathrm{rot,int}}^{\mathrm{EHR}}(T) &= Q_{\mathrm{rot,int}}^{\mathrm{HO}}(T) \sqrt{\frac{\beta}{2\pi}} \sqrt{\left.\frac{\partial^2 V}{\partial \varphi^2}\right|_0} \int_0^{2\pi} f_A(\varphi) \\ &\quad \times f_{\mathrm{vib}}(\varphi,T) e^{-\beta V^{\mathrm{HR}}(\varphi)} d\varphi \\ &= \kappa_{\mathrm{EHR}}(T) Q_{\mathrm{rot,int}}^{\mathrm{HO}}(T). \end{aligned} \tag{47}$$

It turns out that the correction on the HO partition function becomes independent of the absolute value of the (reduced) moment of inertia of the internal rotation under consideration, but only depends on its relative variations.

The increased consistency of the EHR approach is thus reflected in the correction factors f_A and f_{vib} solely. All additional coupling terms originating from rotational-vibrational coupling and Coriolis terms are comprised in these factors.

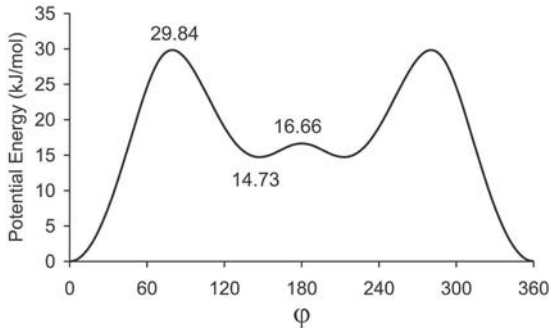

FIG. 1. Potential-energy profile of the φ hindered rotation calculated at the B3LYP/6-311g** level of theory. The reference ($\varphi=0$) is the trans geometry.

C. Relation between HR and EHR

It is instructive to discuss the differences between the proposed coupled-vibrational EHR scheme and the standard 1D-HR scheme.

This can best be visualized by deriving a similar expression as Eq. (47) within the 1D-HR description. The partition function for the specific internal rotation with torsional angle φ *including the Pitzer-Gwin correction factor* can be expressed as

$$Q_\varphi^{\mathrm{HR}} = Q_\varphi^{\mathrm{HO\text{-}QM}} \sqrt{\frac{\beta}{2\pi}} \sqrt{\left.\frac{\partial^2 V}{\partial \varphi^2}\right|_0} \int_0^{2\pi} e^{-\beta V^{\mathrm{HR}}(\varphi)} d\varphi, \tag{48}$$

where $Q_\varphi^{\mathrm{HO\text{-}QM}}$ represents the quantum-mechanical partition function for the torsional motion φ with frequency $\nu = \sqrt{\partial^2 V/\partial \varphi^2|_0 / I^{\mathrm{red}}}$ resulting from the curvature of the potential energy at the equilibrium position and the reduced moment of inertia. It should be stressed that it does not describe an eigenmode, and an inconsistency frequently encountered in the literature consists in replacing the pure HO mode Q_1^{HO} by Q_φ^{HR} of Eq. (48), as discussed in the Introduction.

In a well-implemented 1D-HR model the global partition function has the following final expression:

$$\begin{aligned} Q_{\mathrm{rot,int}}^{\mathrm{1D\text{-}HR}}(T) &= Q_{\mathrm{rot,int}}^{\mathrm{HO}}(T) \sqrt{\frac{\beta}{2\pi}} \sqrt{\left.\frac{\partial^2 V}{\partial \varphi^2}\right|_0} \int_0^{2\pi} e^{-\beta V^{\mathrm{HR}}(\varphi)} d\varphi \\ &= \kappa_{\mathrm{HR}}(T) Q_{\mathrm{rot,int}}^{\mathrm{HO}}(T). \end{aligned} \tag{49}$$

The great similarity of Eqs. (49) and (47) is not a straightforward result, as both models rely on different grounds.

The origin of the success of the 1D-HR method in most of the applications is now clear. The only difference with EHR lies in the presence of the factors $f_A(\varphi)$ and $f_{\mathrm{vib}}(\varphi,T)$ in the integral. The value of these factors at the potential-energy minimum is unity by definition, making the HR and EHR integrands equal at the reference geometry.

The presence of the $f_A f_{\mathrm{vib}}$ factor in the integrand can only have a significant influence on κ_{EHR} when the Boltzmann factor is appreciably different from zero over a large enough range of φ. This can only occur at elevated temperatures or for small potential-energy variations along the large-amplitude path. As a result, the correction of the EHR values versus HR will be small in general.

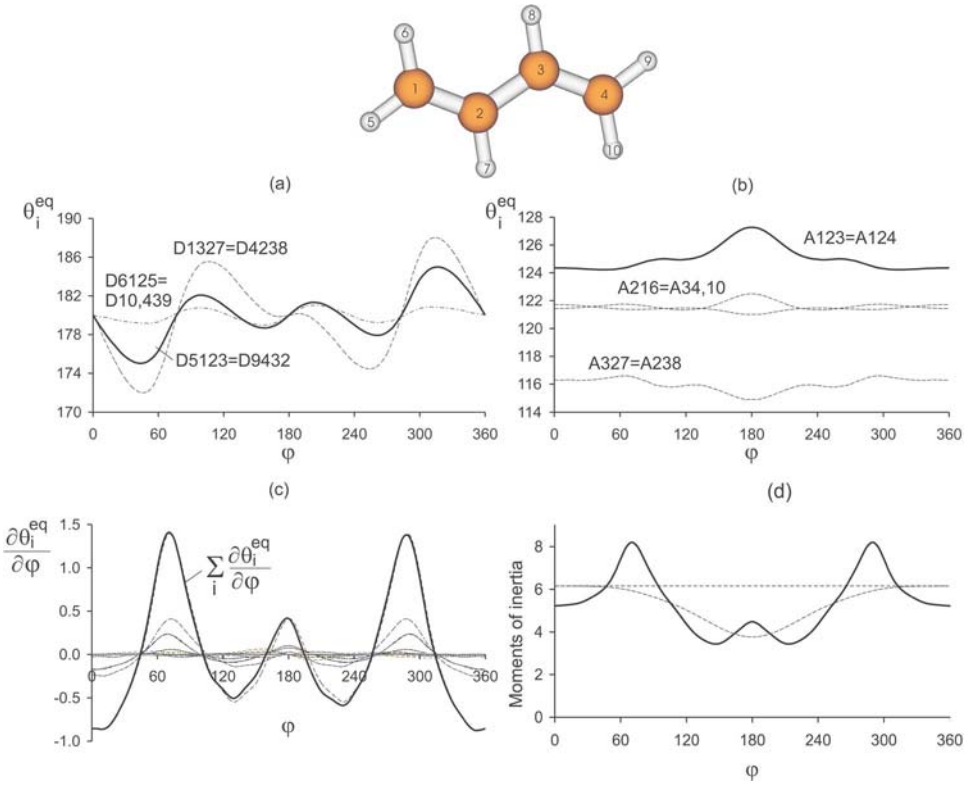

FIG. 2. The influence of the relaxation on the dihedral angles (a) and bond angles (b) is shown as a function of the torsional angle φ. Both dihedral and bond angles are labeled according to the atom numbers as given at the top of the figure. In (c) the summation over the derivatives of the equilibrium angles and bond stretches is displayed (bold black line). Also the individual contributions are plotted. In (d) the resulting EHR moment $A_{\varphi\varphi}$ (black line) is compared with the constant HR moment $A_{\theta_1\theta_1}(\theta_1=0)$ and the varying reduced moment $A_{\theta_1\theta_1}(\theta_1)$ (dotted line). All moments are expressed in units m_{au} Å^2.

In the next sections, we present three examples to illustrate the differences between HR and EHR. The aim is to show the influence of the geometry and vibrational coupling on thermodynamic and kinetic properties. As the partition function itself is not a directly measurable quantity, we have to rely on derived properties. The first two examples employ the entropy and heat capacity, while in the third example the rate constant of an addition reaction is studied. These three quantities sample the partition function, and hence the scaling factor κ_{EHR}, in different ways. The entropy and heat capacity involve derivatives with respect to temperature:

$$S = R\left(\ln Q_{\mathrm{tot}} + T\left(\frac{\partial \ln Q_{\mathrm{tot}}}{\partial T}\right)\right), \tag{50}$$

$$C = RT\left(2\frac{\partial \ln Q_{\mathrm{tot}}}{\partial T} + T\frac{\partial^2 \ln Q_{\mathrm{tot}}}{\partial T^2}\right). \tag{51}$$

Within the formulation of the transition-state theory, the rate constant of a bimolecular reaction can be expressed as follows:[21,22]

$$k(T) = \frac{k_B T}{h}\frac{(q_{\ddagger}/V)}{(q_A/V)(q_B/V)}e^{-\Delta E_0/k_B T}. \tag{52}$$

When an internal rotation is present in the transition state only, the reaction rate becomes proportional to the partition function of interest $(q_{\ddagger})$.

The role of the scaling factor κ_{EHR} in the HR or EHR approach becomes clear when we refer all quantities to their HO solution:

$$S_{\mathrm{EHR}} = S_{\mathrm{HO}} + R\left(\ln \kappa_{\mathrm{EHR}} + T\left(\frac{\partial \ln \kappa_{\mathrm{EHR}}}{\partial T}\right)\right), \tag{53}$$

$$C_{\mathrm{EHR}} = C_{\mathrm{HO}} + RT\left(2\frac{\partial \ln \kappa_{\mathrm{EHR}}}{\partial T} + T\frac{\partial^2 \ln \kappa_{\mathrm{EHR}}}{\partial T^2}\right), \tag{54}$$

$$k_{\mathrm{EHR}}(T) = k_{\mathrm{HO}}(T)\kappa_{\mathrm{EHR}}. \tag{55}$$

III. APPLICATION TO 1,3-BUTADIENE

In a first example the model is applied to 1,3-butadiene, in which only one internal rotation is present about a single CC bond. The one-dimensional hindered-rotor potential is calculated along the lines of Refs. 7 and 8 by pointwise geometry optimizations at fixed out-of-plane angles (5° increments). For each of these constrained optimizations the Hessian was calculated in internal coordinates.

All *ab initio* calculations were performed using the GAUSSIAN 03 software package[20] on the B3LYP/6-311g** (Refs. 23 and 24) level of theory. It should be stressed that the B3LYP method as used here yields highly accurate geometries for the systems under study.[25,26] In addition, this density-functional theory (DFT) also predicts quite reliable quantitative values for the energy barriers in *n*-alkanes.[7] As the primary goal of this numerical application is to test the applicability and efficiency of the proposed EHR model, the proposed level of theory is largely sufficient.[26] The most intensive computational cost lies in the construction of the full Hessian at each point of the rotational potential. The required

computational time is almost double of that needed in a standard 1D-HR calculation, which is more than feasible.

The potential $V^{HR}(\varphi)$ is shown in Fig. 1. In the vicinity of the reference geometry $\varphi=0$, the variation is very steep and results in a barrier of about 30 kJ/mol. Around the *cis* geometry, there is a wide plateau with two shallow minima, lying approximately 15 kJ/mol higher in energy than the reference conformation. This specific energy profile suggests the HO approach to be relatively accurate, as high energies are needed to overcome the large energy barrier towards the energy plateau in the center. At moderate temperatures only a small amount of molecules will reside in the higher-energy conformations.

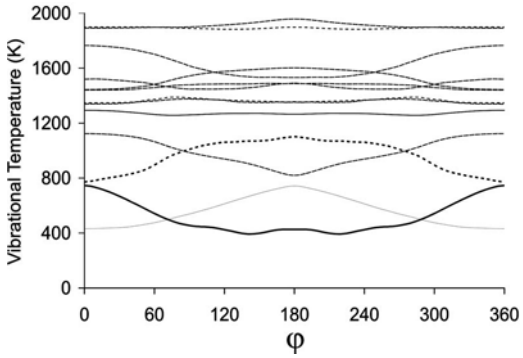

FIG. 3. Vibrational temperature ($\Theta_i=h\nu_i/k_B$) variation of the lowest (up to 2000 K) HO modes in terms of the internal rotation coordinate φ.

A. The scaling factor $\kappa_{EHR}(T)$

The difference of the EHR scaling factor [Eq. (42)] versus the HR approach [Eq. (49)] is completely determined by two correction factors: the geometry factor $f_A(\varphi)$ and the vibrational correction factor $f_{vib}(\varphi,T)$ arising from the other $3N-7$ degrees of freedom.

(i) The geometry factor $f_A(\varphi)$ depends on the variation of the moments of inertia arising from both global and internal rotations. The global moments of inertia I_x, I_y, and I_z turn out to vary very slowly.[8] The behavior of the geometry factor in terms of the torsional angle is thus mostly determined by the reduced moment of inertia $A_\varphi(\varphi)$ [$=A_{\varphi\varphi}$ in Eq. (30)] associated with the internal rotation in the EHR model. The explicit structure of $A_{\varphi\varphi}$ suggests that its magnitude is largely influenced by the relaxation effects, in other words, by the changes of the $3N-7$ other internal degrees of freedom from their equilibrium positions with varying torsional angle φ. To estimate these effects, the variation of the dihedral angles and bond angles along the internal rotation path in the case of 1,3-butadiene is visualized in Figs. 2(a) and 2(b). The bond lengths are not shown as they change little. The largest relaxation values are noticed for the dihedrals (maximum 10°), while the bond angles show rather small variations (maximum 3°). Anyway, the sum of the derivatives of all $(3N-7)$ internal coordinates with respect to the torsional angle [displayed in Fig. 2(c)] shows large fluctuations, and this is the determinative factor in the evaluation of the final EHR moment of inertia [Eq. (30)] and its difference with the 1D-HR reduced moment of inertia. This is best visualized in Fig. 2(d). The dotted line gives the behavior of the A_{θ_1,θ_1} element of the matrix A_Θ [Eq. (30)], which coincides with the constant reduced moment I_m at the reference state.

(ii) The vibrational correction factor $f_{vib}(\varphi,T)$ is even more important than the geometry factor. It shows a temperature dependence, and since thermodynamic functions contain derivatives of the partition function with respect to temperature, this vibrational factor may significantly alter the behavior of the thermodynamic functions. $f_{vib}(\varphi,T)$ [Eq. (44)] is the correction factor arising from the coupling of the IR with the remaining vibrational modes and hence is inherent to the EHR model. These modes are described within the HO approach and as the vibrational partition function is of the form

$$Q^{HO}=\frac{e^{-\Theta^{HO}/2T}}{1-e^{-\Theta^{HO}/T}}, \tag{56}$$

the lowest vibrational temperatures will generate the largest contributions to $\Pi_{i=2}^{n}Q_i^{HO}(\varphi,T)$. In Fig. 3 the fluctuations of the vibrational temperatures Θ_i^{HO} for the vibrational modes are plotted (up to 2000 K) and the most pronounced variations are situated near $\varphi\approx 70°$ and 290°, which are immediately reflected in the behavior of f_{vib} [Fig. 4(a)].

Apparently the shape of the total scaling factor $f_A f_{vib}$ is mainly determined by the vibrational correction factor f_{vib}. For higher temperatures the shape of the function is main-

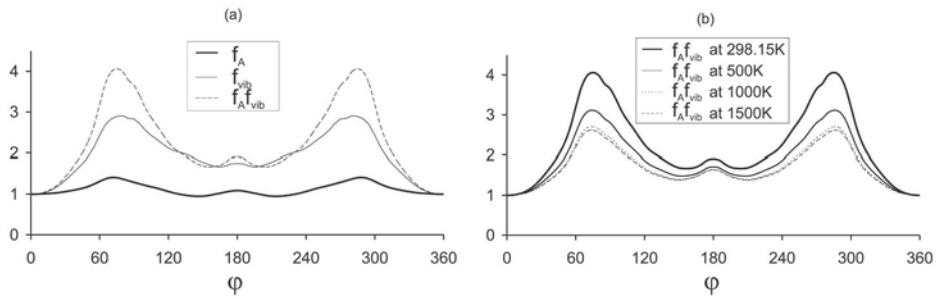

FIG. 4. (a) Variation of the two correction factors f_A and f_{vib} as a function of the torsional angle φ at $T=298.15$ K. (b) Variation of the global correction factor $f_A f_{vib}$ at different temperatures $T=298.15$, 500, 1000, and 1500 K.

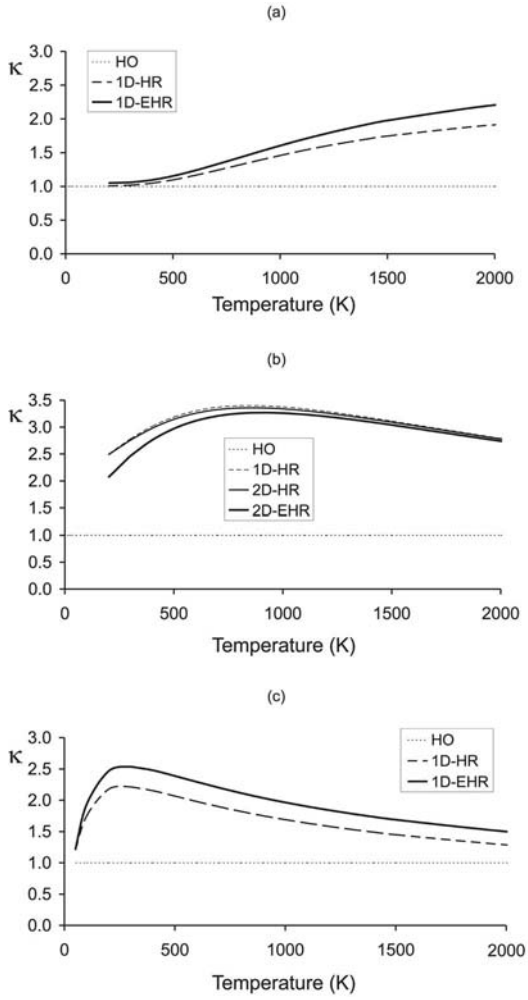

FIG. 5. Scaling factors $\kappa(T)$ for the global partition function in (a) 1,3-butadiene, (b) 1-butene, and (c) the transition state for the addition reaction of a vinyl radical to ethene. The reference is the HO prediction.

tained, but the maxima of the scaling factor are systematically decreasing [Fig. 4(b)]. For very high temperatures the vibrational factor f_{vib} converges to its classical limit. In view of the temperature dependence of f_{vib} we expect the largest corrections on thermodynamic quantities in the lower and intermediate temperature regime. In this particular example validation of the EHR model takes place at the level of the global partition function Q, which comprises complete integration over the dynamics. The scaling factor $\kappa_{\mathrm{EHR}}(T)$, representing the ratio of the EHR prediction with respect to the HO reference, is given in Fig. 5(a). The presence of one hindered rotor in 1,3-butadiene does not give rise to high values of the scaling factor. This is also mainly due to the steep potential around the reference geometry. At room temperature the EHR model predicts a scaling of 1.06, compared with 1.02 in the standard 1D-HR approach.

B. Reproduction of thermodynamic quantities

Experimental validation of EHR is possible with the predicted thermodynamic functions: entropy and heat capacity. In Table I(a) we display the results for these properties in the HO, HR, and EHR models together with the experimental values. The latter are taken from compilations of thermochemical reference data of Yaws[27] and NIST.[28] These reference data often result from fitting measured data from various sources, making the overall accuracy at any single temperature hard to assess. The quoted heat capacities in the compilations,[27,28] for example, can differ by about 2 J/mol/K. One should therefore attach more significance to systematic trends over a wide temperature range, as explained below in connection with Table I(b) and Fig. 7.

Corrections for the entropy arising from the hindered rotor in this specific molecule are expected to be small due to the steep walls of the potential energy around the reference geometry, making the population of other conformers than *trans*-butadiene less probable. Nevertheless, the entropy correction in the EHR model is almost twice as large as the prediction in the 1D-HR model. In molecules with floppier internal rotations, such as *n*-alkanes, the corrections for hindered rotors are much larger as confirmed in Ref. 7.

The heat capacities are more sensitive to the specific model used for the internal motions. To get an idea about the nature, origin, and magnitude of the anharmonic correction to the heat capacity, we plot the contribution to the heat capacity for the specific internal rotation in Fig. 6 as a function of temperature. The heat capacities in the HO model converge to a value of R for higher temperatures, whereas

TABLE I. (a) Comparison of entropy and heat capacity, calculated at the B3LYP/6-311g** level of theory, of the different models with two sets of reference values (Refs. 27 and 28) in 1,3-butadiene. (b) rms and MAD deviations of the calculated heat capacities from experiment for the entire temperature range. All values are given in J/mol/K.

(**a**)	S(298.15 K)	C(100 K)	C(200 K)	C(298.15 K)	C(400 K)	C(600 K)	C(800 K)	C(1000 K)	C(1500 K)
Ref. 27	278.74	39.77	61.01	81.37	101.31	135.02	159.74	175.43	195.87
Ref. 28		41.31	57.14	79.81	103.44	136.51	157.67	173.10	197.54
HO	276.42	40.88	55.47	74.33	94.87	127.63	150.75	167.79	194.52
1D-HR	277.06	40.98	55.84	76.57	99.82	134.69	156.35	171.27	194.38
1D-EHR	277.72	41.64	56.88	78.00	101.65	136.80	158.13	172.62	195.04

(b)	RMS of C(100 K→1500 K)		MAD of C(100 K→1500 K)	
	Ref. 27	Ref. 28	Ref. 27	Ref. 28
HO	6.11	5.90	5.40	5.31
1D-HR	2.84	2.35	2.30	2.17
1D-EHR	2.06	1.31	1.69	1.05

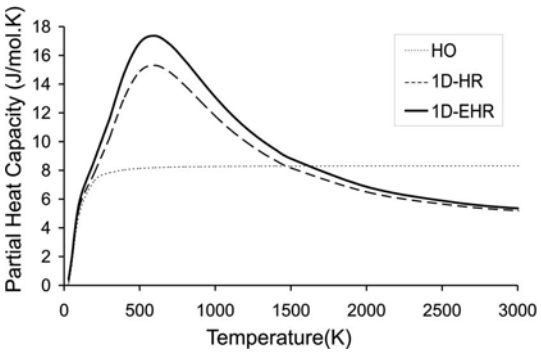

FIG. 6. Partial heat capacity of the internal rotation in the HO, HR, and EHR models. All values are in J/mol/K.

the (E)HR predictions tend to $R/2$. In the lower-temperature regime—the extent of this region is determined by the specific temperature—the IR rotor predictions lie above the HO values. These results are completely in agreement with the results of Katzer and Sax,[29] who studied the impact of anharmonic molecular vibrations in the thermochemistry of silicon hydrides. Also note that the standard anharmonic oscillator correction (using local information about the third-order derivatives at the equilibrium point) does not lead to a significant improvement over the HO, as we have checked explicitly for the applications in this section and the next.

In Figs. 7(a) and 7(b) the absolute deviations of the heat capacities from the reference values (Refs. 27 and 28, respectively) are visualized in terms of the temperature. The HO model systematically underestimates the experimental values at all temperatures, but the deviations are less pronounced for higher temperatures. As shown in Table I(b), the mean absolute deviation (MAD) from both sets of reference values is more than 5 J/mol/K, while the maximal deviation amounts to about 9 J/mol/K.

Changing the HO to a rotational description leads to a substantial improvement and a MAD of less than half the HO value, within the range of acceptable results. However, it is clear that a further systematic and significant improvement is present when going from HR to EHR.

IV. APPLICATION TO 1-BUTENE

In a second example the EHR model is applied to 1-butene, in which two internal rotations are present about single C–C bonds. The theory is easily extended to multiple large-amplitude motions. We are not going into detail, since it is a straightforward extension of the presented theory. The only inconvenience in the numerical application of 2D-EHR is that in a proper EHR model the coupling of the two internal rotations should be strictly taken into account. This causes some increase of the computation time as two-dimensional rotational potential surfaces should be constructed following the lines explained in Refs. 8 and 9. The search for a proper 1D treatment of the two coupled internal rotations within EHR will certainly enlarge the utility and efficiency of the EHR model. Suitable one-dimensional approximation schemes need to be investigated and are requisite for high-dimensional nD-EHR applications ($n>3$). This work is in progress.

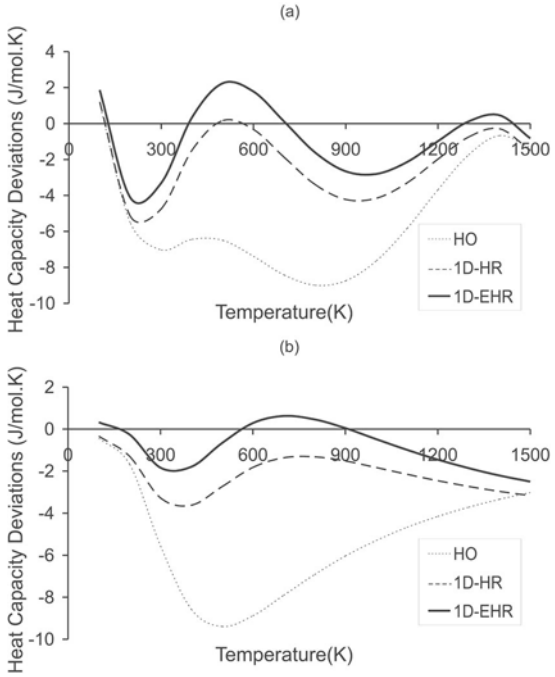

FIG. 7. Deviations from reference values of the heat capacity calculated in the HO, HR, and EHR approaches: compared with (a) Ref. 27 and (b) Ref. 28. All values are in J/mol/K.

The scaling factors $\kappa(T)$ in the various schemes, shown in Fig. 5(b), are noticeably higher than in the case of 1,3-butadiene. The largest correction is predicted by the standard 1D-HR model. Coupling of the two rotations (2D-HR) has only little effect, but an exact treatment of the two internal rotations within the EHR model manifestly reduces the scaling factor. This result gives an indication that the coupling of the IRs with the other vibrational modes in the molecule can give rise to substantial deviations from the standard treatment. It can lead to an increase of the partition function (1,3-butadiene) or a decrease (1-butene). At room temperature an exact EHR calculation causes an enhancement of the total partition function with a factor of 2.45, while in standard hindered-rotor models this factor is larger (2.75–2.78). This deviation is apparently not manifested to the same extent in the reproduction of the thermodynamic functions. The entropy predictions are quite close to the experiment for all schemes handling the hindered rotors, and the same behavior is noticed for the heat capacities with little preference for the 2D-EHR model (see Table II). Concluding, the numerical applications demonstrate that the EHR model, which represents an almost exact treatment of the internal modes in a molecular system, gives nearly similar thermodynamic functions as those predicted by the simple 1D-HR approach. The authors showed in a previous work that the 1D-HR also performs well in the description of multiple (coupled) internal rotations (2D-HR and 3D-HR).[8]

V. APPLICATION TO REACTION KINETICS

To underline the utility and applicability of the EHR model in predicting accurate reaction kinetic parameters, we

TABLE II. Comparison of entropy and heat capacity, calculated at the B3LYP/6-311g** level of theory, of the different models with experiment (Refs. 27 and 28) in 1-butene. All values are given in J/mol/K.

	S(298.15 K)	C(200 K)	C(298.15 K)	C(400 K)	C(600 K)
Ref. 27	307.83	67.55	88.41	109.22	145.84
Ref. 28		65.19	85.56	108.48	146.75
HO	296.97	62.41	82.64	106.30	146.61
1D-HR	307.80	65.46	85.30	107.48	144.68
2D-HR	307.62	65.37	85.27	107.57	144.87
2D-EHR	308.12	66.20	85.93	108.08	145.21

study in this section a particular reaction as an example. More precisely, the rate constant of the addition of the vinyl radical to ethene is investigated (Scheme 2):

Within the formulation of the transition-state theory, the rate constant of a bimolecular reaction can be expressed as follows:[21,22]

$$k(T) = \frac{k_B T}{h} \frac{(q_{\ddagger}/V)}{(q_A/V)(q_B/V)} e^{-\Delta E_0/k_B T}, \tag{57}$$

where k_B represents the Boltzmann constant, T stands for the absolute temperature, h is Planck's constant, and V is the reference volume in which the translational part of the partition function is evaluated. The molecular partition functions q_A and q_B relate to the two reactants and $q_{\ddagger}$ is the molecular partition function of the transition state. ΔE_0 represents the molecular energy difference at absolute zero between the activated complex and the reactants, with inclusion of the zero-point vibrational energies. The frequency factor figuring in the Arrhenius rate law reflects any changes in the molecular partition functions of reactants and products.[19]

For the reaction under study, only one internal rotation is present in the transition state, i.e., a torsion about the forming bond (mode 2 in Fig. 8). Of particular importance in the calculation of the frequency factor are the so-called transitional modes in the transition structure of the reaction. They arise from the loss of three transitional and three rotational degrees of freedom when the reactants combine to form the transition state. The six transitional modes for the vinyl radical addition to ethene are schematically shown in Fig. 8. One of these transitional modes corresponds to the reaction coordinate and is characterized by an imaginary frequency. For a radical addition reaction the latter merely corresponds to the

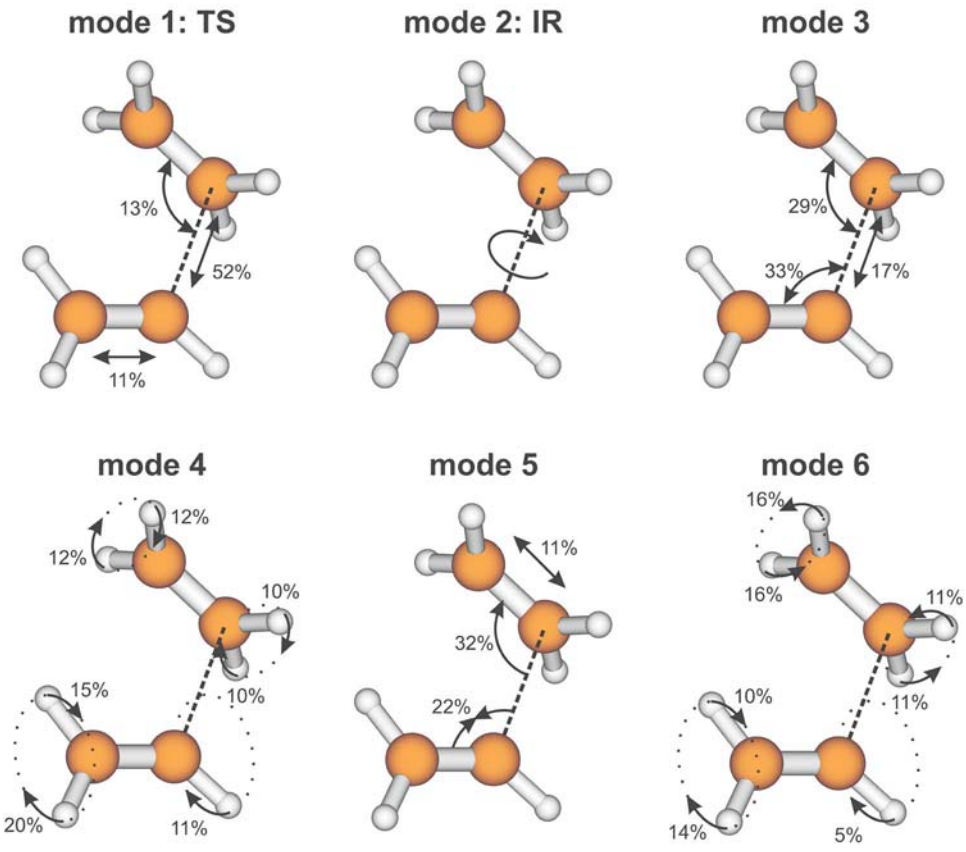

FIG. 8. Schematic representation of the six transitional modes in the transition state for the addition of a vinyl radical to ethene.

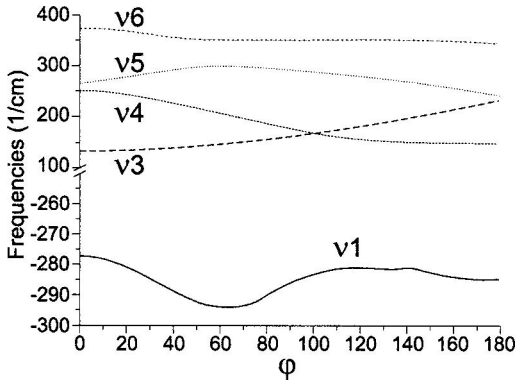

FIG. 9. Variation of the vibrational frequencies (cm^{-1}) of the transitional modes in terms of the dihedral angle of the rotation about the forming C–C bond.

C–C stretch vibration of the forming carbon-carbon bond. Modes 3 and 5 correspond to symmetric and antisymmetric bendings of the two reactant species, whereas ν_4 and ν_6 correspond to symmetric and asymmetric variations of the dihedrals of the hydrogen atoms attached to the carbon backbone with respect to the forming bond.

All normal modes will slightly change in going from reactants to transition state, but due to the specific structure of the ratio $q_{\ddagger}/(q_A)(q_B)$, small changes occurring in the nontransitional modes will approximately cancel. On the other hand, the contributions from the transitional modes will not cancel with respect to any internal mode present in the reactants. The sensitivity of the calculated frequency factor of the model used to treat one internal rotation may thus be reflected in the contributions arising from the transitional modes. Figure 9 shows the variation of the vibrational frequencies of the translational modes in terms of the dihedral angle of the rotation about the forming C–C bond.

The variations in the vibrational modes are significant, i.e., of the order of 100 cm^{-1}. It is generally known that the transitional modes corresponding to the rotation about the forming bond and the bending of the reactant species are important for a radical addition reaction, but the EHR results apparently point towards the importance to incorporate correctly the coupling between the various modes.[18,19] The impact of the coupling is nicely reflected in the scaling factor κ that amounts to about 2.5 in the 1D-EHR model and 2.0 in the standard 1D-HR scheme [see Fig. 5(c)]. As the Arrhenius frequency factor is directly linked to the molecular partition functions, any change in the latter will directly be reflected in the value of A. The Arrhenius plots for the given reaction are shown in Fig. 10. The values for the kinetic parameters, obtained in the temperature range of 300–600 K, are also given for the various approaches.

The activation energy is merely unaffected by any HR scheme in correspondence with previous literature work on this item.[18,30] By taking into account the internal rotation in the transition state, the preexponential factor is approximately doubled. The EHR model induces a slight shift (ca. 17%) in the Arrhenius plot towards higher values.

We also checked that using a different functional (mPW1B95,[31] shown to give both reliable geometries and reaction barriers[32]) leads to the same qualitative difference

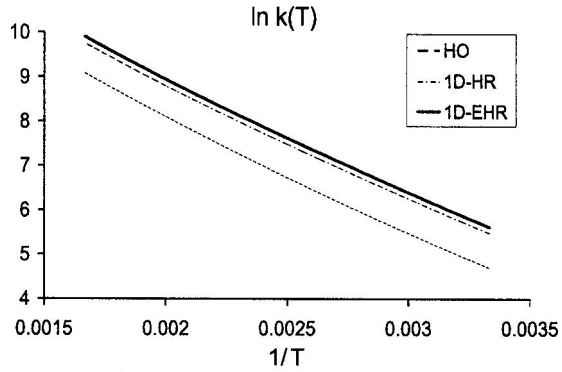

	HO	1D-HR	1D-EHR
E_a	21.98	21.40	21.46
A	6.48 E5	1.16 E6	1.36 E6

FIG. 10. Arrhenius plot of $\ln k$ vs $1/T$ for the addition of the ethyl radical to ethene. The values of E_a are expressed in kJ/mol, whereas the frequency factor A has the dimension of $m^3/mol/s$.

between HR and EHR, i.e., the activation energy remains constant, whereas the preexponential factor increases. More extensive studies on a large database of radical addition reactions are planned to draw definite conclusions about the extent of coupling between various transitional modes and the effect on the kinetic parameters.

VI. SUMMARY

In this paper we have introduced a new model that treats all internal motions, i.e., both large- and small-amplitude vibrations in the molecule, in a unified model. This scheme goes beyond the conventional separability assumption between global and internal motions and between large-amplitude motions and other vibrational degrees of freedom. The approach relies on the introduction of a specific internal coordinate system, in which the global and internal motions can be separated instantaneously at all times such that the Coriolis terms become zero.

In this paper the approach has been elaborated in detail for the case where one internal rotation is present, leading to the extended hindered-rotor (EHR) model in which the relaxation of the other $3N-7$ degrees of freedom are taken into account both in the description of the potential energy and kinetic energy. The finally obtained partition function can be written in its standard harmonic-oscillator form, but multiplied by a scaling factor $\kappa_{\mathrm{EHR}}(T)$, which accounts for all additional coupling with the small-amplitude vibrations. The method is validated by means of the reproduction of thermodynamic and kinetic properties. As a first example 1,3-butadiene is taken, since only one internal rotation is present. Due to the specific form of the internal rotation potential the largest effect is found on the heat capacity, bringing its value to an improved agreement over the whole temperature range as compared with the HR description.

The EHR method is easily extended to more hindered rotors. As a second example 1-butene with two internal rotations has been investigated. It has been shown that the

coupling between the internal rotors and the other vibrations of the molecule causes a substantial reduction of the global partition function compared with the standard 1D-HR model. The applicability of the EHR model to multiple internal rotors enhances the utility of the model. It also gives a reliable alternative to the simple standard 1D-HR approach in molecules where the last method fails. The applicability on reaction kinetics is studied as well: the addition of the vinyl radical to ethene is taken as a third example. Any change in the partition function is directly reflected in the preexponential factor. It is found that the largest influence is already involved in the 1D-HR scheme with respect to the harmonic-oscillator approach, whereas the EHR model causes an additional slight enhancement of the frequency factor.

Finally, we investigated the origin of the success of a well-implemented HR model through its relation with the EHR description. Further refinements of the EHR model with the principal goal to enhance the efficiency of the procedure without losing accuracy are in progress.

ACKNOWLEDGMENTS

This work is supported by the Fund for Scientific Research-Flanders (FWO) and the Research Board of Ghent University.

[1] K. S. Pitzer, J. Chem. Phys. **8**, 711 (1940).
[2] K. S. Pitzer and W. D. Gwin, J. Chem. Phys. **10**, 428 (1942).
[3] K. S. Pitzer, J. Chem. Phys. **14**, 239 (1946).
[4] J. E. Kilpatrick and K. S. Pitzer, J. Chem. Phys. **17**, 1064 (1949).
[5] D. R. Herschbach, H. S. Johnston, K. S. Pitzer, and R. E. Powell, J. Chem. Phys. **25**, 736 (1956).
[6] J. C. M. Li and K. S. Pitzer, J. Phys. Chem. **60**, 466 (1956).
[7] P. Vansteenkiste, V. Van Speybroeck, G. B. Marin, and M. Waroquier, J. Phys. Chem. A **107**, 3139 (2003).
[8] V. Van Speybroeck, P. Vansteenkiste, D. Van Neck, and M. Waroquier, Chem. Phys. Lett. **402**, 479 (2005).
[9] P. Vansteenkiste, V. Van Speybroeck, E. Pauwels, and M. Waroquier, Chem. Phys. **314**, 109 (2005).
[10] M. L. Eidinoff and J. G. Aston, J. Chem. Phys. **3**, 379 (1946).
[11] A. L. L. East and L. Radom, J. Chem. Phys. **106**, 6655 (1997).
[12] P. Y. Ayala and H. B. Schlegel, J. Chem. Phys. **108**, 2314 (1998).
[13] K. Van Cauter, V. Van Speybroeck, P. Vansteenkiste, M. F. Reyniers, and M. Waroquier, ChemPhysChem **7**, 131 (2006).
[14] J. K. G. Watson, Mol. Phys. **15**, 479 (1968).
[15] S. Carter, N. Pinnavaia, and N. C. Handy, Chem. Phys. Lett. **240**, 400 (1995); S. Carter, J. M. Bowman, and L. B. Harding, Spectrochim. Acta, Part A **53**, 1179 (1997); S. Carter, S. J. Culik, and J. M. Bowman, J. Chem. Phys. **107**, 10458 (1997); S. Carter and J. M. Bowman, *ibid.* **108**, 4397 (1998); S. Carter, J. M. Bowman, and N. C. Handy, Theor. Chem. Acc. **100**, 191 (1998); S. Carter and N. C. Handy, J. Chem. Phys. **113**, 987 (2000); D. P. Tew, N. C. Handy, and S. Carter, Mol. Phys. **99**, 393 (2001); D. P. Tew, N. C. Handy, and S. Carter, Phys. Chem. Chem. Phys. **3**, 1958 (2001); D. P. Tew, N. C. Handy, S. Carter, S. Irle, and J. M. Bowman, Mol. Phys. **101**, 3513 (2003).
[16] A. Roitberg, R. B. Gerber, R. Elber, and M. A. Ratner, Science **268**, 1319 (1995); L. Norris, M. A. Ratner, A. Roitberg, and R. B. Gerber, J. Chem. Phys. **105**, 11261 (1996); J. O. Jung and R. B. Gerber, *ibid.* **105**, 10332 (1996); A. Roitberg, R. B. Gerber, R. Elber, and M. A. Ratner, J. Phys. Chem. B **101**, 1700 (1997).
[17] J. Jellinek and D. H. Li, Phys. Rev. Lett. **62**, 241 (1989).
[18] V. Van Speybroeck, D. Van Neck, M. Waroquier, S. Wauters, M. Saeys, and G. B. Marin, J. Phys. Chem. A **104**, 10939 (2000).
[19] J. P. A. Heuts, R. G. Gilbert, and L. Radom, Macromolecules **28**, 8771 (1995); J. P. A. Heuts, R. G. Gilbert, and L. Radom, J. Phys. Chem. **100**, 18997 (1996).
[20] M. J. Frisch, G. W. Trucks, H. B. Schlegel *et al.*, GAUSSIAN 03, Revision B.03, Gaussian, Inc., Pittsburgh, PA, 2003.
[21] K. J. Laidler, *Chemical Kinetics* (Harper Collins, New York, 1987).
[22] D. A. McQuarrie and J. D. Simon, *Physical Chemistry: A Molecular Approach* (University Science, Sausalito, CA, 1997).
[23] A. D. Becke, J. Chem. Phys. **98**, 5648 (1993).
[24] R. Krishnan, J. S. Binkley, R. Seeger, and J. A. Pople, J. Chem. Phys. **72**, 650 (1980).
[25] W. Kohn, A. D. Becke, and R. G. Parr, J. Phys. Chem. **100**, 12974 (1996); M. L. Coote, J. Phys. Chem. A **108**, 3865 (2004).
[26] B. M. Wong and W. H. Green, Mol. Phys. **103**, 1027 (2005).
[27] C. L. Yaws, *Chemical Properties Handbook* (McGraw-Hill, New York, 1999).
[28] NIST Chemistry Webbook: http://webbook.nist.gov/chemistry/
[29] G. Katzer and A. F. Sax, J. Phys. Chem. A **106**, 7204 (2002).
[30] V. Van Speybroeck, D. Van Neck, and M. Waroquier, J. Phys. Chem. A **106**, 8945 (2002).
[31] Y. Zhao and D. G. Truhlar, J. Phys. Chem. A **108**, 6908 (2004).
[32] Y. Zhao and D. G. Truhlar, J. Phys. Chem. A **109**, 5656 (2005).